Research Article

Xiang-Zhen Zhuge[#], Wan-Xiang Hu[#], Yu-Mei Liu, Chang-Yue Jiang, Xiao-Hua Zhang, Meng-Hua Chen, Lu Xie*

PD98059 protects SH-SY5Y cells against oxidative stress in oxygen-glucose deprivation/reperfusion

https://doi.org/10.1515/tnsci-2022-0300 received April 20, 2023; accepted July 11, 2023

Abstract: Mitochondria play a key role in the cerebral ischemia-reperfusion injury. Although the extracellular signal-regulated kinase 1/2 inhibitor PD98059 (PD) is a selective and reversible flavonoid that can protect the mitochondria in a rat model of cardiac arrest/cardiopulmonary resuscitation, its role requires further confirmation. In this study, we investigated whether PD could maintain mitochondrial homeostasis and decrease reactive oxygen species (ROS) production in neuroblastoma (SH-SY5Y) cells exposed to oxygen-glucose deprivation/reperfusion (OGD/R). PD improved the mitochondrial morphology and function, reversed the increase in ROS production and cell apoptosis, and reduced totalsuperoxide dismutase and Mn-superoxide dismutase activities induced by OGD/R. PD decreases ROS production and improves mitochondrial morphology and function, protecting SH-SY5Y cells against OGD/R-induced injury.

Keywords: extracellular signal-regulated kinase, oxidative stress, mitochondria, apoptosis

co-first author.

Xiang-Zhen Zhuge, Wan-Xiang Hu, Xiao-Hua Zhang: Department of Physiology, Pre-Clinical Science, Guangxi Medical University, 22 Shuangyong Road, Nanning, 350001, Guangxi, China

Yu-Mei Liu: Shenzhen Bay Laboratory Neuropathy Institute of China, Shenzhen, 518107, Guangdong, China

Chang-Yue Jiang: Department of Pharmacy, HIV/AIDS Clinical Treatment Center of Guangxi (Nanning) and The Fourth People's Hospital of Nanning, Nanning, 530000, China

Meng-Hua Chen: Institute of Cardiovascular Diseases, The Second Hospital Affiliated to Guangxi Medical University, Nanning, 530000, Guangxi, China, e-mail: cmhnn@sina.com

1 Introduction

Cardiac arrest (CA) is a global health problem, accounting for 20% of all deaths in Western countries [1]. Brain injury after cardiopulmonary resuscitation (CPR) eventually leads to death [2]. A series of complex pathophysiological processes, including disordered energy metabolism, oxidative stress, mitochondrial injury, inflammation, and calcium overload, are involved in cerebral ischemia-reperfusion injury (CIRI) [3–5]. Studies on the mechanisms underlying CIRI will help improve prognosis and reduce mortality. Extracellular-regulated protein kinase (ERK) is activated by oxidative stress [6] and ischemia [7]. One study found that chromium caused an increase in reactive oxygen species (ROS) generation, ERK activation, and mitochondrial damage in SH-SY5Y cells, and PD improved its oxidative stress and mitochondrial dysfunction [8]. Dexmedetomidine and resveratrol have been shown to inhibit transient focal CIRI in rats [7,9]. Previously, we showed that PD98059 (PD), a specific ERK inhibitor, ameliorated oxidative stress and mitochondrial injury-related apoptosis and autophagy in a rat model of CA/CPR, conferring cerebral and renal protection [10-12]. Furthermore, antioxidative tea polyphenols and epigallocatechin gallate have been shown to alleviate CIRI in a dose-dependent manner via inhibition of ERK and modulation of mitochondrial function [13,14]. In an in vitro study, PAQR3 abated oxygen-glucose deprivation/reperfusion (OGD/R)-induced injury by suppressing ERK signaling in N2a cells [15]. Based on these findings, here, we established an SH-SY5Y model of OGD/R and evaluated mitochondrial morphology and function, oxidative stress, and cell apoptosis to further reveal the protective effects of PD.

2 Materials and methods

2.1 Cell culture and treatment groups

Human neuroblastoma SH-SY5Y cells were obtained from the China Center for Type Culture Collection (Wuhan, China).

^{*} Corresponding author: Lu Xie, Department of Physiology, Pre-Clinical Science, Guangxi Medical University, 22 Shuangyong Road, Nanning, 350001, Guangxi, China, e-mail: xielu8282@163.com, tel: +86-13707885560; fax: +86-7715352775

They were verified to be of the correct lineage and uncontaminated by other cell types or organisms. The cells were cultured in a mixed substrate, comprising a 1:1 mixture of Minimal Essential Medium (MEM) and F12 (Gibco BRL, Gaithersburg, MD, USA) and 10% fetal bovine serum (Gibco BRL) at 37°C under 5% CO₂.

SH-SY5Y cells were stochastically separated into five groups as follows: normal control group (control), DMSO (solvent for PD) control group (DMSO), OGD/R group, PD low-dose group (PD 10 μ mol/L, PD-L), and PD high-dose group (PD 20 μ mol/L, PD-L).

2.2 OGD/R model

The OGD/R model was established as previously described [16]. For the OGD/R procedure, SH-SY5Y cells were cultured in glucose-free and serum-free Dulbecco's modified Eagle medium (DMEM) in an incubator with 100% $\rm N_2$ to maintain the oxygen concentration around <0.1% at 37°C for 5 min. Following different periods of OGD (1, 2, and 3 h), ischemic–hypoxic cells were re-incubated in MEM/F12 medium at 37°C under 5% $\rm CO_2$ for 24 h.

2.3 Determination of cell viability

Cell viability was determined using a CCK-8 cell counting kit (Dojindo, Kyushu, Japan) following the manufacturer's instructions. The cells were seeded in 96-well plates at 2 \times 10^5 cells/mL and incubated for 24 h. Six wells were used for each treatment and control group. After OGD/R, a mixture of 90 μL of DMEM and 10 μL of CCK-8 was added to each well. The absorbance of the samples at 450 nm was measured following incubation at 37°C for 2.5 h in the dark.

2.4 ROS measurement

Intracellular ROS levels were determined using the 2,7-dichlorofluorescein diacetate (DCFH-DA) fluorescence probe (Beyotime Biotechnology, Shanghai, China). Following treatment, the cells were collected and incubated with 0.1% DCFH-DA in DMEM at 37°C for 20 min. The cells were then washed three times with serum-free DMEM. DCFH fluorescence was recorded in three randomly selected fields. The experiment

was repeated three times. The intensity of DCFH fluorescence was assessed using ImageI Pro Plus 6.0 (Media Cybernetics).

2.5 Measurement of total superoxide dismutase (T-SOD) and Manganese-superoxide dismutase (SOD) activities

SOD activity was determined using a SOD assay kit (Nanjing Jiancheng Bioengineering Institute, Nanjing, China) according to the manufacturer's protocol. The cells were seeded in sixwell plates at 1×10^6 cells/well and incubated for 24 h. The cells were then lysed in ice-cold RIPA buffer for 30 min. After centrifugation at $12,000\times g$ for 15 min at 4°C , the supernatant was collected. Protein levels were assessed using a BCA protein assay kit (Beyotime Biotechnology). The Cu/Zn-SOD level in the supernatant was determined according to the manufacturer's instructions. The absorbance of the samples at 550 nm was measured using an ultraviolet spectrophotometer (Youke T2602, Youke Instrument, Shanghai, China).

2.6 Detection of mitochondrial membrane potential (MMP)

MMP was examined using a fluorescent probe kit (Beyotime Biotechnology). Briefly, the cells were cultured in six-well plates with JC-1 dye working solution for 20 min at 37°C and then washed twice with JC-1 staining solution. The medium was added to each well. Red (JC-1 aggregates) and green (JC-1 monomer) fluorescence were recorded in three randomly selected fields. Fluorescence intensity was estimated using Image J Pro Plus 6.0.

2.7 Observation of mitochondrial structure

The cells were treated with 4% glutaraldehyde at 4°C for 1 h, rinsed twice with pre-cooled phosphate-buffered saline (PBS), and then treated with 1% OsO_4 for 1 h. The samples were dehydrated with 50% ethanol, 70% ethanol, 80% ethanol, 90% ethanol, 90% ethanol:90% acetone (1:1), 90% acetone, and 100% acetone three times for 10 min per step, and then incubated at 25°C for 1 h. The samples were then embedded in epoxy resin, placed at 35°C for 15 h, then at 45°C for 12 h, and finally at 60°C for 24 h. The cell masses

were cut into ultrathin slices and stained. The mitochondrial structure was observed using transmission electron microscopy (Hitachi, Tokyo, Japan), and three different fields were captured.

2.8 Determination of apoptosis using Hoechst 33258 staining

Apoptosis was evaluated using a Hoechst 33258 staining kit (Beyotime Biotechnology). The cells were harvested, washed, mixed with 4% (v/v) paraformaldehyde at 25°C for 30 min, further washed, and stained with 500 µL of Hoechst 33258 for 5 min. Fluorescence microscopy (LI-COR, Lincoln, NE, USA) was used to observe nuclear morphology.

2.9 Determination of apoptosis using flow cytometry

Apoptosis was measured using flow cytometry with Annexin V-fluorescein isothiocyanate (FITC) and propidium iodide (PI). Early apoptosis of cells was detected by binding Annexin V to phosphatidylserine exposed laterally. PI is a nucleic acid dye that cannot pass through normal cells with intact cell membranes and early apoptotic cells but can pass through the cell membranes of middle and late apoptotic cells and necrotic cells to stain the nucleus. The kit (Beyotime Biotechnology) uses Annexin V combined with PI to distinguish cells at different stages of apoptosis. Flow cytometric analyses were performed using a BD FACSCalibur Flow Cytometer (BD Biosciences; San Jose, CA, USA). Briefly, the cells were seeded in six-well plates at 1×10^6 cells/well. After treatment, the cells were harvested and rinsed twice with PBS. The cells were stained with a 1:1 mixture of V-FITC and PI for 15 min under dark conditions. Thereafter, 400 µL of Annexin V binding buffer was added to each well. Finally, apoptosis was measured using flow cytometry after 1 h.

2.10 Western blotting

The cells were lysed in cold RIPA buffer with a 1% protease inhibitor cocktail and phenylmethylsulfonyl fluoride for 30 min. After centrifugation at 13,000×g for 15 min at 4°C, the supernatant was collected. Protein expression was measured using a BCA protein assay kit. Identical amounts of protein were loaded into a sodium dodecyl-sulfatepolyacrylamide gel electrophoresis gel and transferred onto a polyvinylidene fluoride membrane. The membrane was blocked in 5% bovine serum albumin for 1 h and then incubated with primary antibodies against phosphor-extracellular-regulated protein kinase 1/2 (p-ERK1/2, 1:2,000), cleavedcaspase 3 (1:500), caspase 3 (1:500), Bax (1:2,000), Bcl-2 (1:500), Drp-1 (1:500), Mfn1 (1:1,000), Opa1 (1:1,000), and Cyto C (1:500) at 4°C overnight. All the primary antibodies were purchased from Cell Signaling Technology. Thereafter, the membrane was incubated with an IRDye800CW-coupled secondary antibody at 25°C for 2 h. Finally, the membranes were visualized using a western blotting detection system with the Li-Cor Odyssey Scanner imaging densitometer (Li-Cor Biosciences, Lincoln, NE, USA), and the assessed bands were quantitated using the ImageJ Pro Plus 6.0. software.

2.11 Statistical analysis

Statistical analyses were performed using SPSS software 22.0. Values are presented as mean value ± standard deviation. The Kolmogorov-Smirnov test was used to test for normality and equal variance. All data were processed using a one-way analysis of variance. Results with p <0.05 were considered significant.

3 Results

3.1 Cellular morphology and cell viability after different durations of oxygen and glucose deprivation (OGD)

Neuroblastoma SH-SY5Y cells were subjected to OGD for 1, 2, and 3 h, followed by reoxygenation for 24 h. Inverted phase-contrast microscopy was used to determine cellular morphology. With prolonged OGD, the number of adherent cells decreased, whereas the number of floating cells increased (Figure 1a). This suggests that OGD markedly affected the morphology of SH-SY5Y cells.

Cell viability was assessed using a CCK-8 kit, according to the manufacturer's instructions. Compared with that of the control group (100% ± 0.33%), cell viability decreased with prolonged OGD, as follows: $81\% \pm 0.17\%$ at 1 h, 56% \pm 0.25% at 2 h, $35\% \pm 0.14\%$ at 3 h, and $26\% \pm 0.10\%$ at 4 h. Considering an optimal cellular density of 50-60% for drug evaluation, cells were subjected to OGD of 2h in the subsequent experiments (Figure 1b).

3.2 ROS levels and p-ERK and ERK expression

Redox imbalance is a key factor in the development of CIRI. ROS production was determined in SH-SY5Y cells using fluorescence microscopy. The fluorescence intensity was as follows: normal control (control) (101.30 ± 11.48), dimethyl sulfoxide (DMSO) control (DMSO) (137.43 ± 10.89), OGD/R (378.01 ± 45.10), PD low dose (PD-L) (248.69 ± 37.75), and PD high dose (PD-H) (201.99 ± 10.78). OGD/R increased the ROS levels compared with the control (p < 0.01). However, treatment with PD reversed these changes (Figure 2a and b). This indicated that oxidative stress is involved in OGD/R. As shown in Figure 2c, the p-ERK and p-ERK/ERK levels increased in the OGD/R group (p < 0.01 vs the control group) but decreased in the PD-H group (p < 0.05 vs the OGD/R group) (Figure 2c and d).

3.3 Detection of T-SOD and Mn-SOD activities

SOD is a key intracellular antioxidant, and Mn-SOD is an essential mitochondrial antioxidant enzyme. The activities of both T-SOD and Mn-SOD were lower in the OGD/R group than in the control group (p < 0.01). The Mn-SOD activity increased in both PD-L and PD-H groups than in the OGD/R group (Figure 3).

3.4 Mitochondrial morphology

Mitochondrial ultrastructure was observed under an electron microscope. Intact mitochondrial membranes and

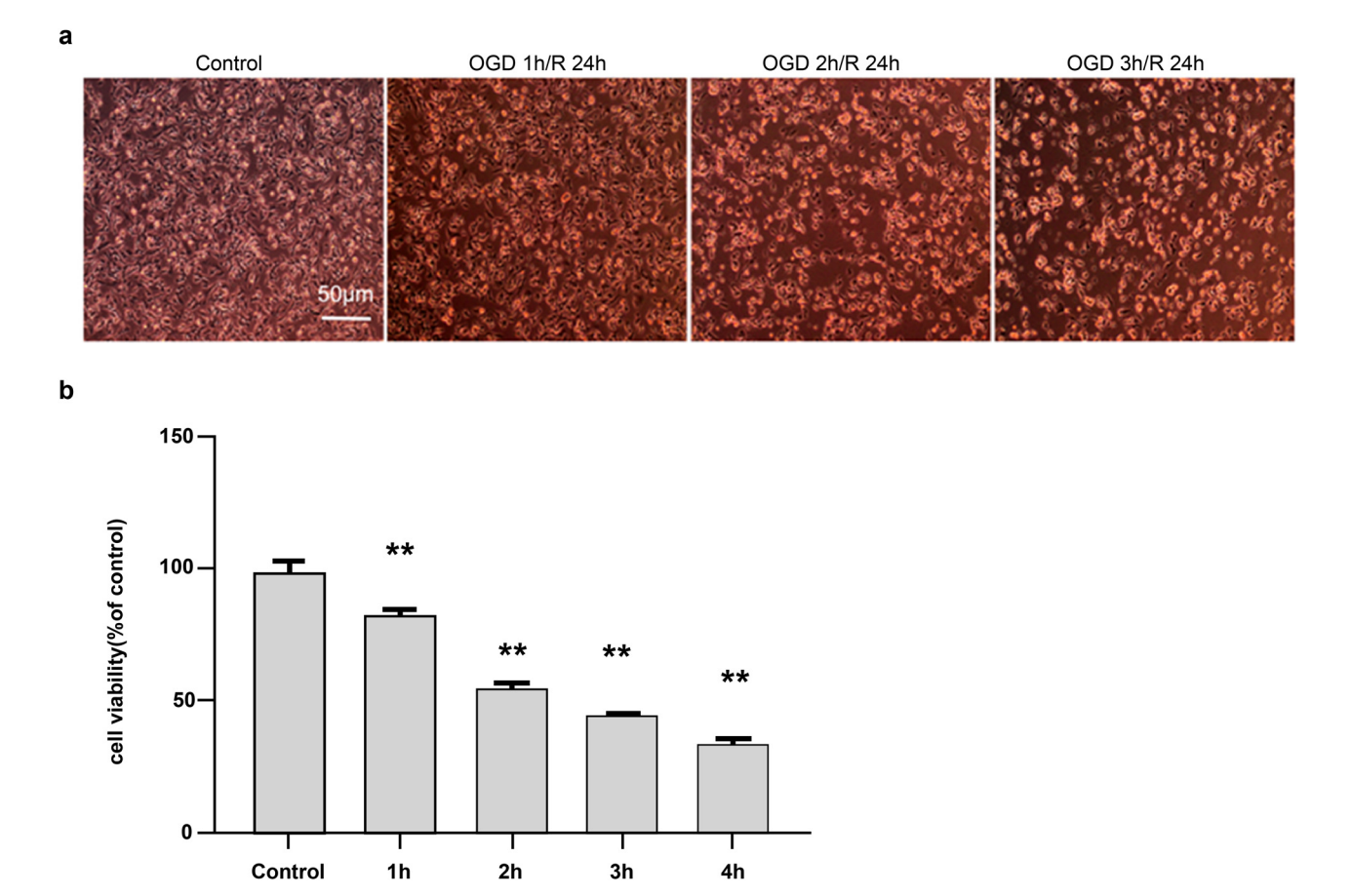


Figure 1: Effect of different durations of oxygen and glucose deprivation (OGD) on cellular morphology and viability. (a) Cellular morphology after different durations of OGD (100×). The morphology of SH-SY5Y cells was observed under an inverted phase-contrast microscope, which revealed a gradual increase in floating cells following OGD. (b) Comparison of cellular viability after different durations of OGD, measured using the CCK-8 method. Scores are presented as mean value \pm standard deviation (n = 5). **p < 0.01 vs the control group.

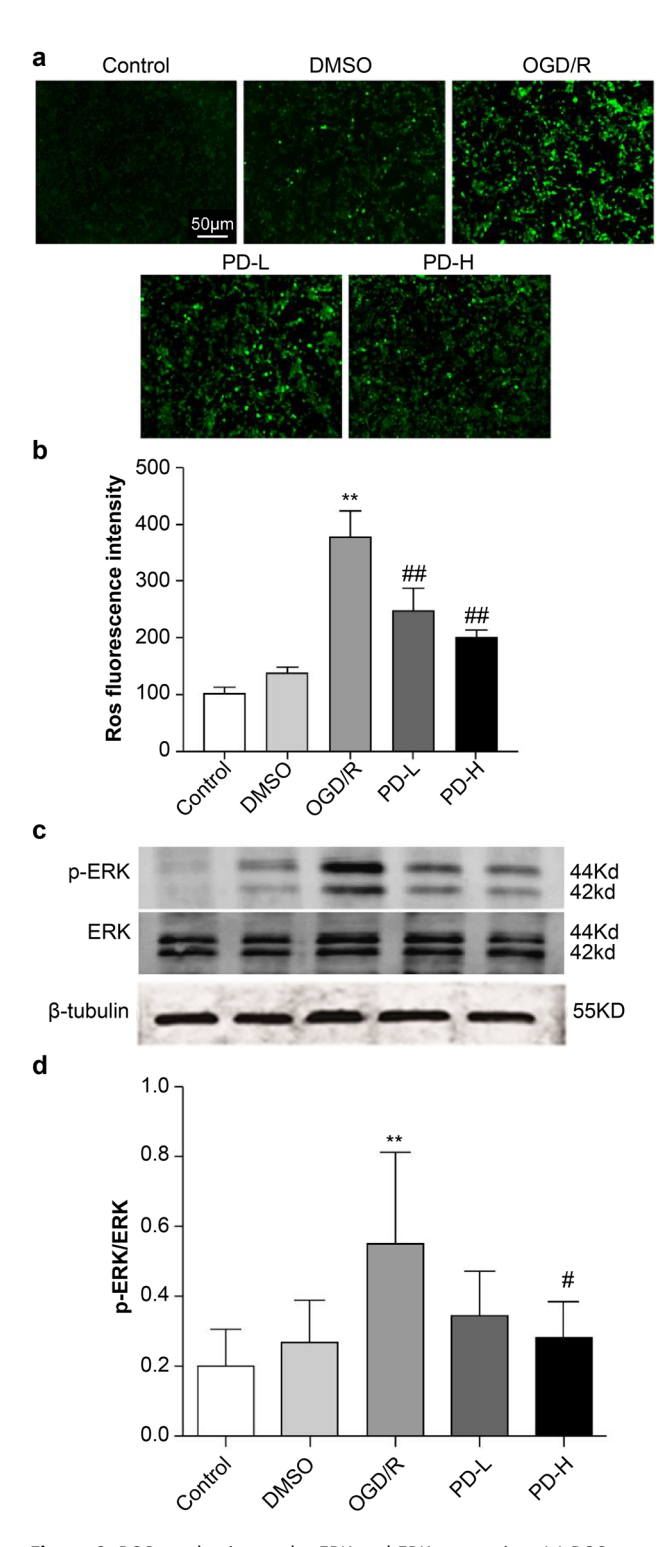


Figure 2: ROS production and p-ERK and ERK expression. (a) ROS fluorescence. (b) ROS fluorescence density. (c) Western blot of p-ERK and ERK. (d) The ratio of p-ERK/ERK. Data are expressed as mean value \pm standard deviation (n=3). **p<0.01 vs the control group; **p<0.01 vs the oxygen–glucose deprivation/reperfusion (OGD/R) group.

clear cristae were observed in the control group. Conversely, swollen mitochondria, broken cristae, and vacuolated matrices

were observed in the OGD/R group. In the PD-L and PD-H groups, broken cristae and vacuolization improved compared with those in the OGD/R group (Figure 4).

Mitochondrial images were obtained under an electron microscope at 50,000×. Arrows indicate a single mitochondrion.

3.5 MMP

A double immune marker was used to evaluate MMP. Red staining indicated a higher potential, whereas green staining indicated a lower potential, denoting early-stage apoptosis. The red and red/green ratios of the OGD/R group decreased compared with those in the control group (p < 0.01), indicating lower MMP levels. A significant enhancement was observed in the MMP in the PD-H group compared with that in the OGD/R group (p < 0.05) (Figure 5).

3.6 Measurement of optic atrophy 1 protein (Opa1), mitofusin 1 (Mfn1), and dynamin-related protein 1 (Drp1) levels

Western blotting was performed to analyze Opa1, Mfn1, and Drp1 levels, which mediate mitochondrial fusion and fission. OGD/R increased Opa1 expression compared with the control (p < 0.01). Opa1 expression decreased considerably in the PD-L and PD-H groups compared with that in the OGD/R group (p < 0.01) (Figure 6a and b). Compared with the control, OGD/R also significantly increased the expression of Mfn1. Both PD-L and PD-H groups showed a downward trend in Mfn1 expression (Figure 6c and d). Compared with the control, OGD/R increased p-Drp1/Drp1, whereas PD-L and PD-H had the opposite effect (Figure 6e and f).

3.7 Hoechst staining and flow cytometry analysis of cell apoptosis

No significant differences in nuclear morphology were observed in the DMSO group compared with that in the control group; however, in the OGD/R group, the staining pattern was dispersed and deep, indicating that the nuclei were disrupted. Compared with OGD/R, PD-L and PD-H significantly improved nuclear morphology (Figure 7a).

Flow cytometry was performed to investigate the effect of PD on apoptosis after OGD/R. The rates of apoptosis were 6 — Xiang-Zhen Zhuge et al. DE GRUYTER

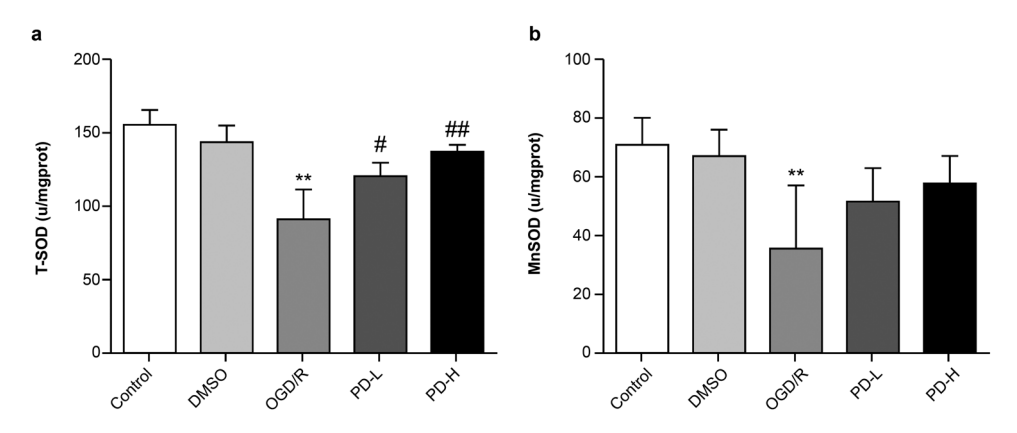


Figure 3: T-SOD and Mn-SOD activities in each group. (a) T-SOD activity. (b) Mn-SOD activity. Data are expressed as mean value \pm standard deviation (n = 3). **p < 0.01 vs the control group; **p < 0.05 vs the OGD/R group; **p < 0.01 vs the OGD/R group.

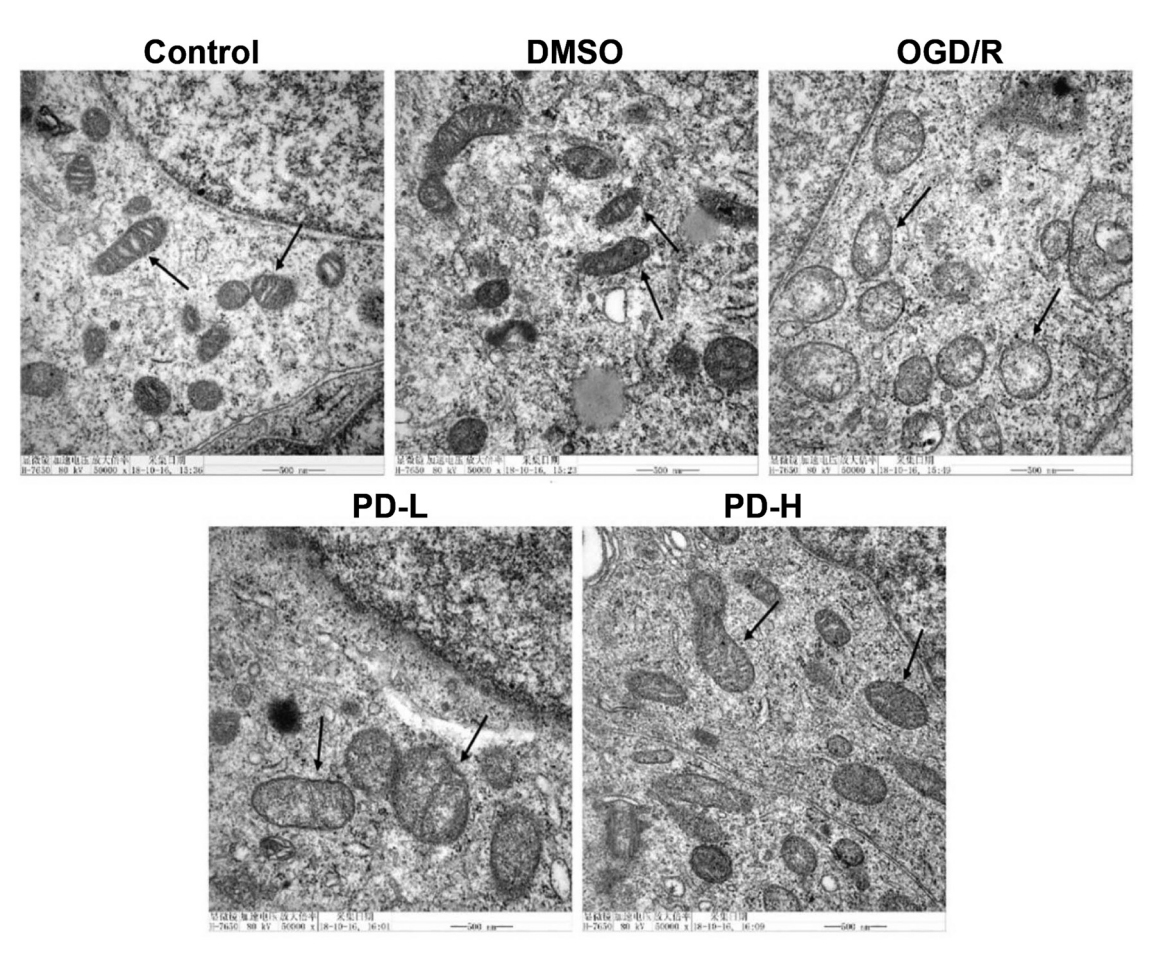


Figure 4: Mitochondrial morphology observed using transmission electron microscopy.

as follows: control group, $8.5\% \pm 5.2\%$; DMSO group, $13.4\% \pm 5.8\%$; OGD/R group, $50.4\% \pm 10.7\%$; PD-L group, $37.6\% \pm 1.1\%$; and PD-H group, $27.9\% \pm 4.6\%$. Both PD-L and PD-H decreased the rate of apoptosis compared with OGD/R (p < 0.05 and p < 0.01, respectively) (Figure 7c).

3.8 Cytochrome C (Cyto C), caspase 3, cleaved-caspase 3, Bax, and Bcl-2 expression

The release of Cyto C from the mitochondria to the cytosol is a critical marker of mitochondrial membrane permeability

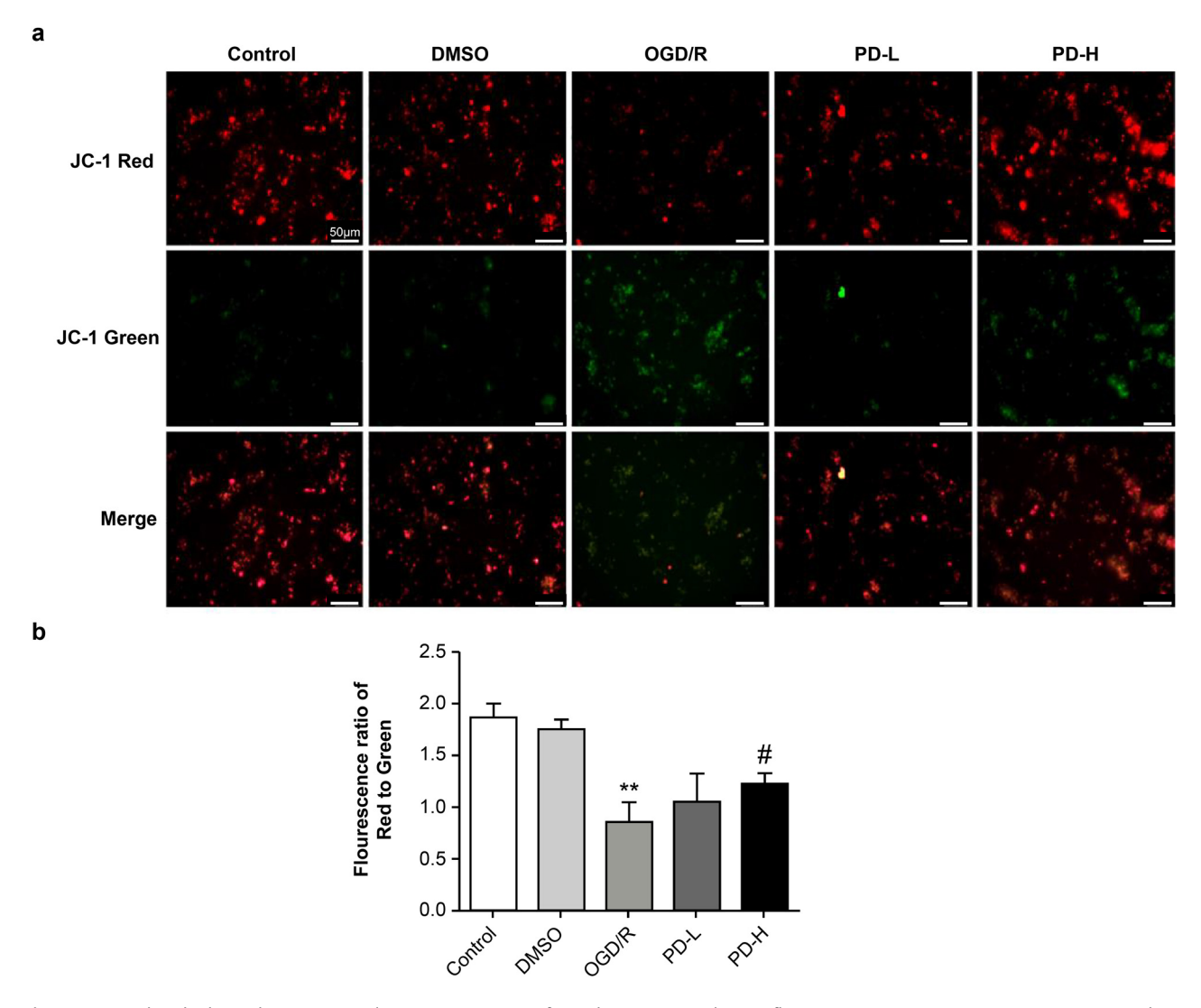


Figure 5: Mitochondrial membrane potential. (a) Determination of membrane potential using fluorescence microscopy. Images were acquired at $100 \times$. (b) The relative amount of red/green fluorescence was calculated using ImageJ software. Data are presented as mean value \pm standard deviation (n = 3). **p < 0.01 vs the control group; *p < 0.5 vs the OGD/R group.

and mitochondria-pathway apoptosis. We found that OGD/R increased Cyto C expression, whereas this was inhibited by PD (Figure 8). The levels of cleaved-caspase-3 and Bcl-2/Bax in the OGD/R group were considerably higher than those in the control group (p < 0.05). PD-H lowered the cleaved-caspase-3 level compared with OGD/R (p < 0.01), and both PD-L and PD-H increased the Bcl-2/Bax level compared with OGD/R (p < 0.05) and p < 0.01, respectively) (Figure 8).

4 Discussion

This study proved that the ERK inhibitor PD reduced ROS production, maintained mitochondrial morphology and function,

and alleviated the mitochondria-dependent apoptosis in SH-SY5Y cells caused by OGD/R. Brain injury following CA/CPR remains a major concern worldwide. The findings of our previous study indicated that PD plays a brain-protection role in a rat model of CA/CPR [12]. To explore the effect of PD *in vitro*, we established an OGD/R model and found that PD alleviated the ROS production following OGD/R injury, mitochondrial injury, and apoptosis in SH-SY5Y cells.

Oxidative stress is an important pathological factor that increases with the changes in mitochondrial function during CIRI [17]. Oxygen deficiency inactivates the mitochondrial proteins of the electron transfer chain, resulting in proton leakage. Following reperfusion, protons react with O_2 , resulting in the overproduction of ROS [18,19]. Inactivation or overconsumption of endogenous antioxidative

DE GRUYTER

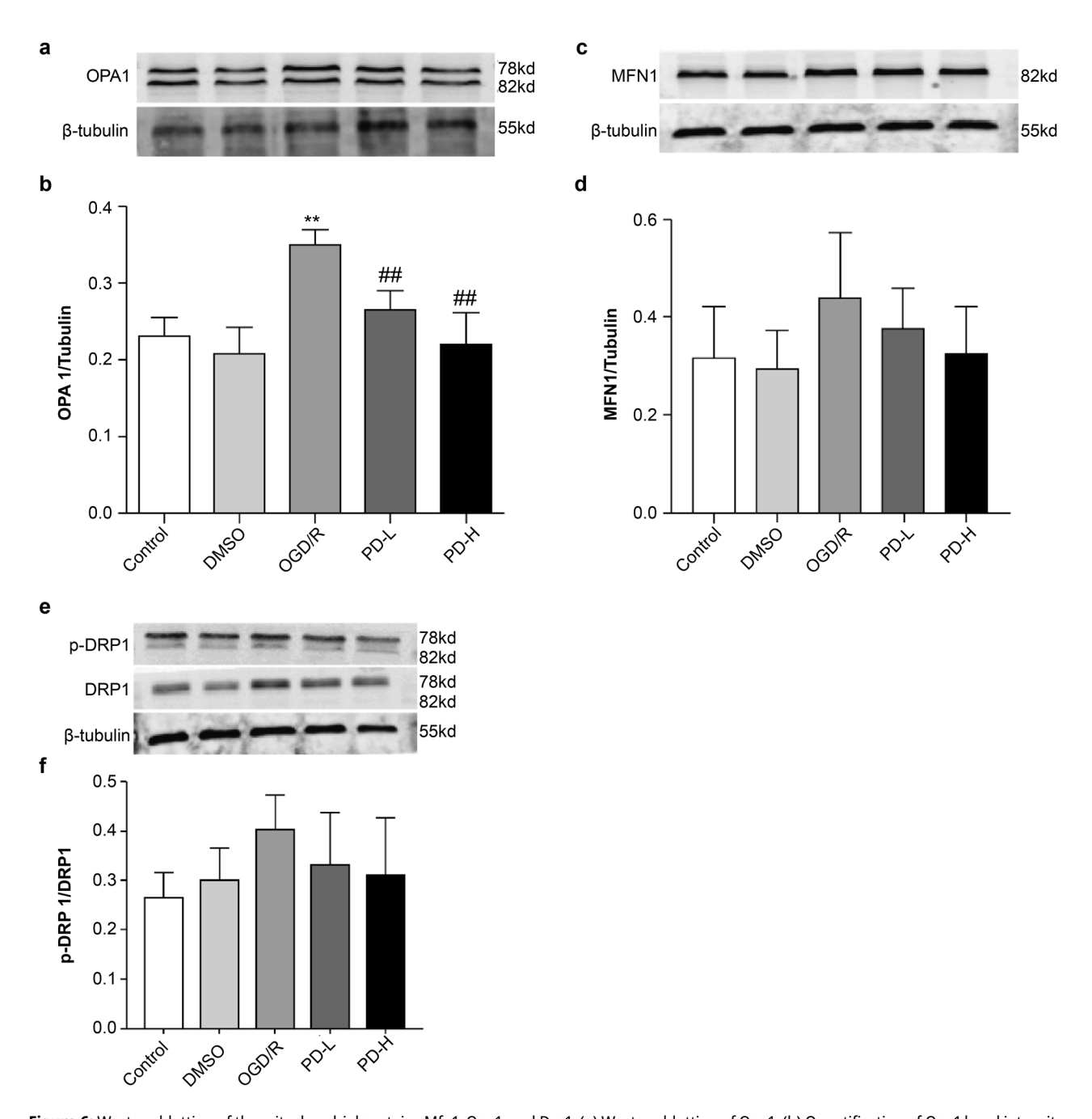


Figure 6: Western blotting of the mitochondrial proteins Mfn1, Opa1, and Drp1. (a) Western blotting of Opa1. (b) Quantification of Opa1 band intensity. (c) Western blotting of Mfn1. (d) Quantification of Mfn1 expression. (e) Western blotting of the mitochondrial fission proteins p-Drp1 and Drp1. (f) Ratio of p-Drp1/Drp1 expression. Overall data are expressed as mean value \pm standard deviation (n = 3). **p < 0.01 vs the control group; **p < 0.01 vs the OGD/R group.

enzymes promotes ischemia-reperfusion injury [2]. Therefore, in this study, PD prevented OGD/R-induced ROS production and Mn-SOD inactivation by protecting the mitochondria. This is consistent with our previous findings: PD plays an antioxidant role via a decrease in ROS production and an increase in the SOD level in a rat model of CA/CPR [20].

Mitochondrial function plays a vital role in cellular fate. Mitochondria-dependent apoptosis is common during ischemia-reperfusion [21,22]. MMP depends on membrane ion transporters, which are sensitive to ischemia. A decrease in MMP, an important index of mitochondrial dysfunction and a hallmark of early apoptosis [23], leads to the transformation of apoptosis-promoting proteins, including Cyto C,

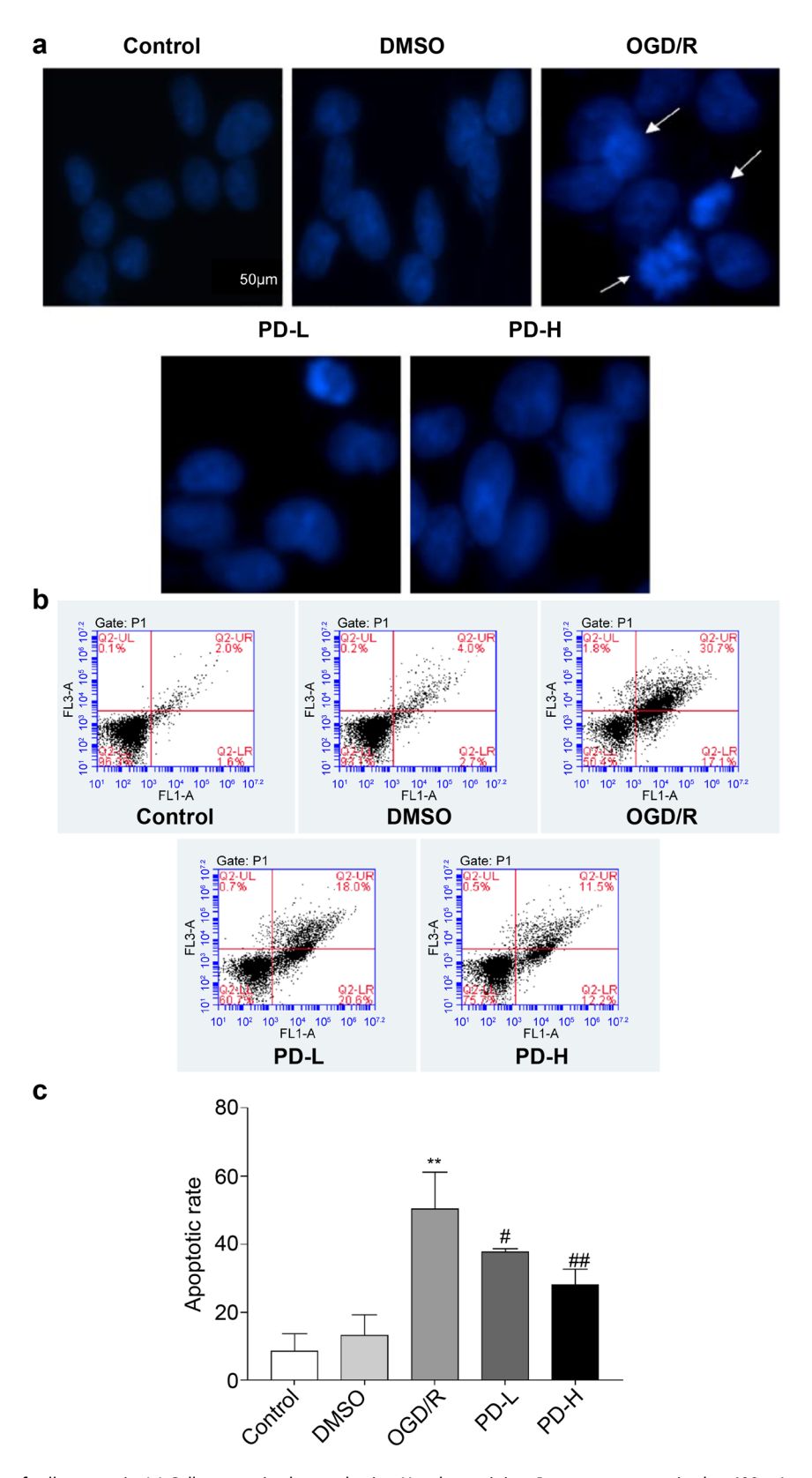


Figure 7: Observation of cell apoptosis. (a) Cell apoptosis observed using Hoechst staining. Images were acquired at 400×. Arrows indicate damaged nuclei. (b and c) The rate of apoptosis was determined using flow cytometry. Data are presented as mean value \pm standard deviation (n = 3). **p < 0.01vs the control group; p < 0.05 vs the OGD/R group; p < 0.01 vs the OGD/R group.

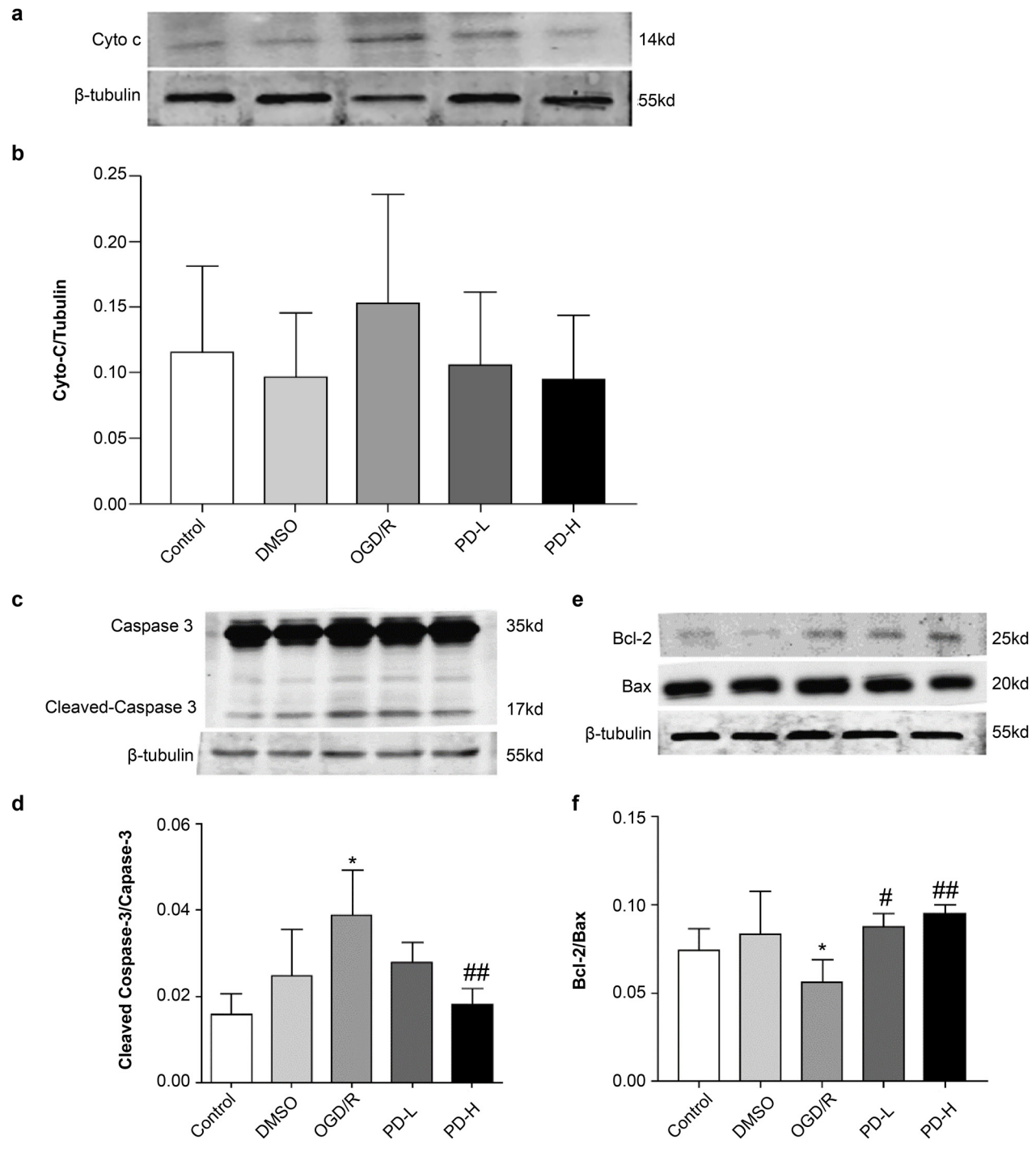


Figure 8: Western blotting of mitochondrial Cyto C, cleaved-caspase 3, caspase 3, Bcl-2, and Bax. (a) Western blotting of Cyto C. (b) Quantification of Cyto C band intensities. (c) Western blotting of cleaved-caspase 3 and caspase 3. (d) Ratio of cleaved-caspase 3/caspase 3 band intensities. (e) Western blotting of Bcl-2 and Bax. (f) Bcl-2/Bax quantification. Values are presented as mean value \pm standard deviation (n = 3). *p < 0.05 vs the control group; *p < 0.05 vs the OGD/R group; *p < 0.05 vs the OGD/R group.

further activating apoptotic Bax and cleaved-caspase-3 [24,25]. In this study, PD improved the mitochondrial ultrastructure, increased MMP, reduced Cyto C release, and downregulated Bax and cleaved-caspase-3 expression.

Mitochondria are highly dynamic, exhibiting fusion and fission [26,27]. Mitochondrial fusion allows the exchange and connection of mitochondrial contents to form normal mitochondria, regulated by Mfn1, Mfn2, and Opa1. Mitochondrial

fission, which is a requisite for cell growth and division, results in sufficient numbers of mitochondria, eliminates impaired mitochondria, and is mainly regulated by Drp1. Experiments have shown that mitochondrial fusion and fission are involved in regulating apoptosis. Silencing Mfn, Opa1, and Drp1 upregulates or downregulates the sensitivity of mitochondria to apoptotic stimuli [28-30]. Several studies have reported that mitochondrial dynamics are imbalanced following CIRI [31,32]. Modulation of the mitochondrial fusion/ fission balance positively affects brain injury. Pretreating a rat model of CIRI with a mitochondrial fusion promoter increases the expression of Mfn1 and reduces the dysfunction and apoptosis of brain mitochondria [32]. Resveratrol acts on the AMPK-Mfn1 pathway to exert antioxidative and antiapoptotic effects in N2a cells subjected to hypoxia-reoxygenation injury. PD upregulates Mfn2, downregulates P-Drp1, and positively labels P-Drp1/TUNEL cells in the cerebral cortex of CA/CPR rats [11,12]. A Drp1 inhibitor (Mdivi-1) or siRNA has been shown to inhibit the mitochondria-dependent apoptotic pathway following cerebral ischemia or CA [30,33]. Drp1 knockdown protects mouse N2a cells against mitochondrial damage and apoptosis during OGD [34]. In this study, SH-SY5Y cells subjected to OGD/R presented increased levels of Opa1, Drp1, and Mfn1, which were reversed by PD. This likely reflected the condition at 24 h of reperfusion due to fluctuating mitochondrial dynamics during ischemia-reperfusion injury. Liu et al. [35] revealed that the expression of Opa1 and Drp1 increased in mouse ischemic penumbra 90 min after transient middle cerebral artery occlusion, followed by a fastigium at 2 days, whereas the expression of P-Drp1 gradually increased, peaking at 14 days. Experimental results may vary among different models depending on the duration and severity of cerebral ischemia.

Although an emerging effect was observed in the total expression of Opa1, Mfn1, and Drp1, the number of western blot repeats was low, which is a limitation of the current study. Thus, dynamic variations in Opa1, Mfn1, and Drp1 levels require observation from multiple time points; however, this report only observed the expression of these proteins during OGD of 2 h.

5 Conclusion

Collectively, our results indicate that the ERK inhibitor PD protected SH-SY5Y cells from OGD/R damage by reducing ROS production, maintaining mitochondrial morphology and function, and alleviating mitochondria-dependent apoptosis. The present findings, together with those of our previous studies in CA/CPR rats, imply that the ERK inhibitor and mitochondrial may be the potential therapeutic target in CIRI.

Acknowledgements: This research was supported by the National Natural Science Foundation of China (nos. 81860333 and 81660312).

Funding information: This work was supported by the National Natural Science Foundation of China (nos. 81860333 and 81660312). The funder plays an important role in writing the paper.

Author contributions: All authors contributed to the study's conception and design. Material preparation, data collection, and analysis were performed by X.Z., W.H., and Y.L. The first draft of the manuscript was written by X.Z. All authors commented on previous versions of the manuscript. All authors read and approved the final manuscript.

Conflict of interest: Authors state no conflict of interest.

Data availability statement: The datasets generated during and/or analyzed during the current study are available from the corresponding author on reasonable request.

References

- Wong CX, Brown A, Lau DH, Chugh SS, Albert CM, Kalman JM, et al. Epidemiology of sudden cardiac death: global and regional perspectives. Heart Lung Circulation. 2019 Jan;28(1):6-14.
- Cui R, Liu S, Wang C, Liu T, Ren J, Jia Y, et al. Methane-rich saline alleviates CA/CPR brain injury by inhibiting oxidative stress, microglial activation-induced inflammatory responses, and ER stress-mediated apoptosis. In: Angelone T, editor. Oxidative medicine and cellular longevity. Vol. 2020, 2020 Oct. p. 1-13.
- Kalogeris T, Baines CP, Krenz M, Korthuis RJ. Ischemia/reperfusion. [3] In: Terjung R, editor. Comprehensive physiology. 1st edn. Wiley; 2016. p. 113-70.
- [4] Yin F, Zhou H, Fang Y, Li C, He Y, Yu L, et al. Astragaloside IV alleviates ischemia reperfusion-induced apoptosis by inhibiting the activation of key factors in death receptor pathway and mitochondrial pathway. J Ethnopharmacol. 2020 Feb;248:112319.
- Zhang YP, Zhang Y, Xiao ZB, Zhang YB, Zhang J, Li ZQ, et al. CFTR prevents neuronal apoptosis following cerebral ischemia reperfusion via regulating mitochondrial oxidative stress. J Mol Med. 2018 Jul;96(7):611-20.
- Su D, Ma J, Zhang Z, Tian Y, Shen B. Protective effects of UCF-101 on cerebral ischemia-reperfusion (Cir) is depended on the MAPK/p38/ ERK signaling pathway. Cell Mol Neurobiol. 2016 Aug;36(6):907-14.
- Zhu YM, Wang CC, Chen L, Qian LB, Ma LL, Yu J, et al. Both PI3K/Akt [7] and ERK1/2 pathways participate in the protection by dexmedetomidine against transient focal cerebral ischemia/reperfusion injury in rats. Brain Res. 2013 Feb;1494:1-8.

- [8] Fu SC, Liu JM, Lee KI, Tang FC, Fang KM, Yang CY, et al. Cr(VI) induces ROS-mediated mitochondrial-dependent apoptosis in neuronal cells via the activation of Akt/ERK/AMPK signaling pathway. Toxicol In Vitro. 2020;65:104795.
- [9] Chang C, Zhao Y, Song G, She K. Resveratrol protects hippocampal neurons against cerebral ischemia-reperfusion injury via modulating JAK/ERK/STAT signaling pathway in rats. J Neuroimmunol. 2018 Feb:315:9–14.
- [10] Fu ZY, Wu ZJ, Zheng JH, Li N, Lu JY, Chen MH. Edaravone ameliorates renal warm ischemia-reperfusion injury by downregulating endoplasmic reticulum stress in a rat resuscitation model. Drug Des Devel Ther. 2020 Jan;14:175–83.
- [11] Zheng JH, Xie L, Li N, Fu ZY, Tan XF, Tao R, et al. PD98059 protects the brain against mitochondrial-mediated apoptosis and autophagy in a cardiac arrest rat model. Life Sci. 2019 Sep;232:116618.
- [12] Zheng JH, Chen MH, Fu ZY, Li N, Xie L. Pd98059 protects cerebral cortex mitochondrial structure and function at 48 h post-resuscitation in a rat model of cardiac arrest. Drug Des Devel Ther. 2020 Dec;14:1107–15.
- [13] Hu W, Wang H, Shu Q, Chen M, Xie L. Green tea polyphenols modulated cerebral SOD expression and endoplasmic reticulum stress in cardiac arrest/cardiopulmonary resuscitation rats. BioMed Res Int. 2020 Feb;2020:1–9.
- [14] Zhuo X, Xie L, Shi FR, Li N, Chen X, Chen M. The benefits of respective and combined use of green tea polyphenols and ERK inhibitor on the survival and neurologic outcomes in cardiac arrest rats induced by ventricular fibrillation. Am J Emerg Med. 2016 Mar;34(3):570–5.
- [15] Peng W, Mo X, Li L, Lu T, Hu Z. PAQR3 protects against oxygenglucose deprivation/reperfusion-induced injury through the ERK signaling pathway in N2A cells. J Mol Hist. 2020 Jun;51(3):307–15.
- [16] Zhang LM, Zhang DX, Zhao XC, Sun WB, Jiang XJ. Sevoflurane preconditioning increases phosphorylation of ERK1/2 and HO-1 expression via inhibition of mPTP in primary rat cortical neurons exposed to OGD/R. J Neurol Sci. 2017 Jan;372:171–7.
- [17] Huang P, Wu SP, Wang N, Seto S, Chang D. Hydroxysafflor yellow A alleviates cerebral ischemia reperfusion injury by suppressing apoptosis via mitochondrial permeability transition pore. Phytomedicine. 2021 May;85:153532.
- [18] Cadenas S. ROS and redox signaling in myocardial ischemiareperfusion injury and cardioprotection. Free Radic Biol Med. 2018 Mar;117:76–89.
- [19] Zhao J, Zhang J, Liu Q, Wang Y, Jin Y, Yang Y, et al. Hongjingtian injection protects against myocardial ischemia reperfusioninduced apoptosis by blocking ROS induced autophagic- flux. Biomed Pharmacother. 2021 Mar;135:111205.
- [20] Nguyen Thi PA, Chen MH, Li N, Zhuo XJ, Xie L. Pd98059 protects brain against cells death resulting from ROS/ERK activation in a cardiac arrest rat model. Oxid Med Cell Longev. 2016;2016:1–13.

- [21] Cai H, Tao X, Zheng L, Huang L, Peng Y, Liao R, et al. Ozone alleviates ischemia/reperfusion injury by inhibiting mitochondrion-mediated apoptosis pathway in SH-SY5Y cells. Cell Biol Int. 2020 Apr;44(4):975–84.
- [22] McBride HM, Neuspiel M, Wasiak S. Mitochondria: more than just a powerhouse. Curr Biol. 2006 Jul;16(14):R551–60.
- [23] Singh MH, Brooke SM, Zemlyak I, Sapolsky RM. Evidence for caspase effects on release of cytochrome c and AIF in a model of ischemia in cortical neurons. Neurosci Lett. 2010 Jan;469(2):179–83.
- [24] Manzanero S, Santro T, Arumugam TV. Neuronal oxidative stress in acute ischemic stroke: Sources and contribution to cell injury. Neurochem Int. 2013 Apr;62(5):712–8.
- [25] Song YH, Cai H, Zhao ZM, Chang WJ, Gu N, Cao SP, et al. Icariin attenuated oxidative stress induced-cardiac apoptosis by mitochondria protection and ERK activation. Biomed Pharmacother. 2016 Oct;83:1089–94.
- [26] Mitra K. Mitochondrial fission-fusion as an emerging key regulator of cell proliferation and differentiation: Prospects & Overviews. BioEssays. 2013 Nov;35(11):955–64.
- [27] Westermann B. Mitochondrial fusion and fission in cell life and death. Nat Rev Mol Cell Biol. 2010 Dec;11(12):872–84.
- [28] Olichon A, Baricault L, Gas N, Guillou E, Valette A, Belenguer P, et al. Loss of OPA1 perturbates the mitochondrial inner membrane structure and integrity, leading to cytochrome c release and apoptosis. J Biol Chem. 2003 Mar;278(10):7743–6.
- [29] Sugioka R, Shimizu S, Tsujimoto Y. Fzo1, a protein involved in mitochondrial fusion, inhibits apoptosis. J Biol Chem. 2004 Dec;279(50):52726–34.
- [30] Li Y, Wang P, Wei J, Fan R, Zuo Y, Shi M, et al. Inhibition of Drp1 by Mdivi-1 attenuates cerebral ischemic injury via inhibition of the mitochondria-dependent apoptotic pathway after cardiac arrest. Neuroscience. 2015 Dec;311:67–74.
- [31] Gao J, Wang H, Li Y, Li W. Resveratrol attenuates cerebral ischaemia reperfusion injury via modulating mitochondrial dynamics homeostasis and activating AMPK-Mfn1 pathway. Int J Exp Path. 2019 Oct;100(5–6):337–49.
- [32] Surinkaew P, Apaijai N, Sawaddiruk P, Jaiwongkam T, Kerdphoo S, Chattipakorn N, et al. Mitochondrial fusion promoter alleviates brain damage in rats with cardiac ischemia/reperfusion injury. JAD. 2020 Sep;77(3):993–1003.
- [33] Kumar R, Bukowski MJ, Wider JM, Reynolds CA, Calo L, Lepore B, et al. Mitochondrial dynamics following global cerebral ischemia. Mol Cell Neurosci. 2016 Oct;76:68–75.
- [34] Tang J, Hu Z, Tan J, Yang S, Zeng L. Parkin protects against oxygen-glucose deprivation/reperfusion insult by promoting Drp1 degradation. Oxid Med Cell Longev. 2016;2016:1–10.
- [35] Liu W, Tian F, Kurata T, Morimoto N, Abe K. Dynamic changes of mitochondrial fusion and fission proteins after transient cerebral ischemia in mice. J Neurosci Res. 2012 Jun;90(6):1183–9.